ROMANIAN JOURNAL OF INFORMATION SCIENCE AND TECHNOLOGY
Volume **13**, Number 1, 2010, 73–83

Spatial Filtering Using Analog Parallel Architectures and Their Log-Domain Implementation

Liviu GORAŞ[1,2], Ion VORNICU[1]

[1]Technical University *Gheorghe Asachi*, Faculty of Electronics, Telecommunications and Information Technology, Iaşi, Romania
[2]Institute of Computer Science, Romanian Academy, Iaşi Branch, Romania
E-mail: {lgoras, ivornicu}@etc.tuiasi.ro

Abstract. A class of linear continuous in time and discrete in space homogeneous Cellular Neural Network type analog parallel architectures and log-domain CMOS implementation is discussed. The specific feature of the spatio-temporal dynamics of the architecture is the existence of unstable spatial modes – property that can be used for high speed image processing. The dynamics and spatial frequency response of a 1D array at system level and log-domain transistor level implementation are compared.

Key words: Cellular Neural Networks, spatio-temporal dynamics, CMOS log-domain implementations.

1. Introduction

Spatio-temporal dynamics in homogeneous or nonhomogeneous arrays have been thoroughly studied in various fields including autonomous Cellular Neural Networks (CNN's) [1–8]. The reasons of the above investigations were, on the one hand, the interest in understanding and modeling natural behaviors and, on the other hand, the possibility of using spatio-temporal dynamics in parallel architectures for high speed signal and image processing. Even though CNN's have been initially designed as intrinsically nonlinear systems, in many cases linear or piecewise versions proved to be useful from the analysis, the design, and the application points of view. As an example, pattern formation, which has been shown to appear, among others, in

an architecture consisting of two-port second order cells, sandwiched between two resistive grids [6, 7] was studied using the powerful linear methods based on the decoupling technique. Even though the method is valid only for the central linear part of the cell characteristics, it has been shown to offer useful insight on the shape of final pattern obtained after the nonlinearity has been reached. It consists of a change of variable chosen according to the boundary conditions, the transformed differential equations being decoupled. When at least one of the spatial modes is unstable, a time variable spatial filter can be obtained in the hypothesis that the outputs did not surpass the central linear part of the cell characteristic. A similar approach proved useful for spatial filtering using more general structures as it will be shown in the next section. Indeed the two-grid coupled CNN is a rather special case of homogeneous parallel architecture, derived from the reaction-diffusion model proposed by Turing. The basic idea of having arrays with one or several bands of unstable spatial modes can be implemented using a more flexible architecture. If the emerging pattern is frozen before the signals leave the central linear part of the cell characteristics, the architecture behaves like a spatial time variable filter, the spatial frequency response being dependent on the moment the transient has been stopped [10, 11].

2. The architecture

In the following, we consider an M cell 1D array with the architecture shown in Fig. 1, generalizations to 2D being straightforward. The array consists of linear cells characterized by the admittances Y(s) and coupled using voltage controlled current sources over a neighborhood N_r of radius r. The template elements have been denoted by A_k for inter-cell connections and by B_k for the input connections. The neighborhood dimension has been chosen the same for both cases, a fact that does not restrict the generality as any of the template coefficients might be zero.

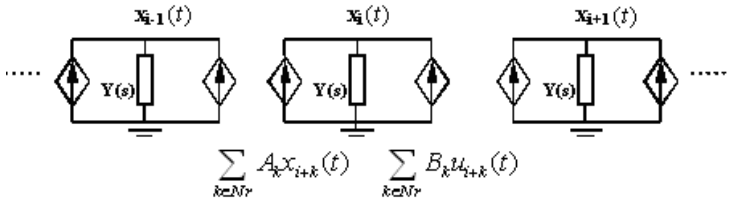

Fig. 1. 1D architecture.

In the following we briefly review the general theory of such arrays and then discuss transistor level implementations.

With the usual notation $s \leftrightarrow d/dt$, $Y(s)$ is a linear integro-differential operator of the form:

$$Y(s) = \frac{Q(s)}{P(s)} = \frac{\sum_{l=0}^{q} q_l s^l}{\sum_{n=0}^{p} p_n s^n}. \tag{1}$$

In this case, the equations that describe the network are:

$$Y(s)x_i(t) = \sum_{k \in Nr} A_k x_{i+k}(t) + \sum_{k \in Nr} B_k u_{i+k}(t). \tag{2}$$

The above relations represent a set of *coupled* integro-differential equations, which can be solved by the decoupling technique using the change of variables:

$$\begin{cases} x_i(t) = \sum\limits_{m=0}^{M-1} \Phi_M(i,m)\hat{x}_m(t) \\ \\ u_i(t) = \sum\limits_{m=0}^{M-1} \Phi_M(i,m)\hat{u}_m(t) \end{cases}, \tag{3}$$

where the M functions $\Phi_M(i,m)$ satisfy the boundary conditions and are orthogonal with respect to the scalar product in C^M. For ring boundary conditions $\Phi_M(i,m)$ have the form $\Phi_M(i,m) = \mathrm{e}^{\mathrm{j}2\pi mi/M} = \mathrm{e}^{j\omega_m i} = \mathrm{e}^{j\omega_0 mi}$, where $\omega_0 = 2\pi/M$ and $\omega_m = 2\pi m/M = \omega_0 m$.

When $\Phi_M(i+k,m) = \mathrm{e}^{\mathrm{j}2\pi mk/M}\Phi_M(i,m)$, which happens in the case of $\Phi_M(i,m) = \mathrm{e}^{\mathrm{j}2\pi mi/M}$, the action of the spatial operators A and B on $\Phi_M(i,m)$ gives:

$$\begin{cases} \sum\limits_{k \in N_r} A_k \Phi_m(i+k,m) = K_A(m)\Phi_m(i,m) \\ \\ \sum\limits_{k \in N_r} B_k \Phi_m(i+k,m) = K_B(m)\Phi_m(i,m) \end{cases}, \tag{4}$$

where

$$K_A(m) = \sum_{k=-r}^{r} A_k e^{j2\pi mk/M},\ K_B(m) = \sum_{k=-r}^{r} B_k e^{j2\pi mk/M}. \tag{5}$$

Thus $\Phi_M(i,m)$ are eigenfunctions of the spatial operators represented by the A and B templates and $K_A(m)$ and $K_B(m)$ are the corresponding spatial eigenvalues which are complex in general and depend on the parameters of the template and on the mode. For symmetric templates, $A_{-k} = A_k$, the spatial eigenvalues are real:

$$K_A(m) = -A_0 + \sum_{k=1}^{r} A_k \cos\frac{2\pi mk}{M}, \tag{6}$$

$$K_B(m) = -B_0 + \sum_{k=1}^{r} B_k \cos\frac{2\pi mk}{M}. \tag{7}$$

In particular, for $r = 2$,

$$K_A(m) = -A_0 + 2A_1 \cos\omega m + 2A_2 \cos 2\omega m, \tag{8}$$

with similar expressions for $K_B(m)$.

Using the above change of variable and the properties of $\Phi_M(i,m)$, equations (2) can be written in the symbolic form:

$$Q(s)\hat{x}_m(t) = K_A(m)P(s)\hat{x}_m(t) + K_A(m)P(s)\hat{u}_m(t), \tag{9}$$

which represent a set of *decoupled* differential equations one for each of the M spatial modes, the new variables being the amplitudes of the spatial modes of the cell signals.

The characteristic polynomial for the m-th mode is:

$$R(s) = Q(s) - K_A(m)P(s). \tag{10}$$

Thus, the stability and dynamics of the spatial modes will depend both on the A-template eigenvalues and on the cell admittance $Y(s) = Q(s)/P(s)$. The spatio-temporal dynamics of the array can be studied using classical methods from feedback/control theory such as the root locus and Nyquist criterion and, of course, the Routh-Hurwitz test, all valid for each of the spatial modes. Analysis of arrays with nonsymmetrical templates can be handled similarly.

For the particular case $Y(s) = s + 1$ we obtain the following set of decoupled autonomous first order differential equations:

$$\frac{d\hat{x}_m(t)}{dt} = (-1 + K_A(m))\hat{x}_m(t), \quad m = 0...M-1 \tag{11}$$

The roots of the m-th characteristic equation are $s_m = -1 + K_A(m)$, where for second order neighborhood $K_A(m)$ has the expression (8).

The roots of $K_A(m) = 0$ represent the intersection of the dispersion curve with the abscissa axis in the hypothesis of a continuous variation of m.

For the above particular case of an autonomous CNN having the cell impedance represented by an RC parallel circuit, the (first order) differential equation corresponding to mode m has the form:

$$C\frac{d\hat{x}_m(t)}{dt} = (K_A(m) - G)\hat{x}_m, \quad m = 0...M-1 \tag{12}$$

where $K_A(m)$ represents the dispersion curve which, for first and second order neighborhoods has the forms mentioned above.

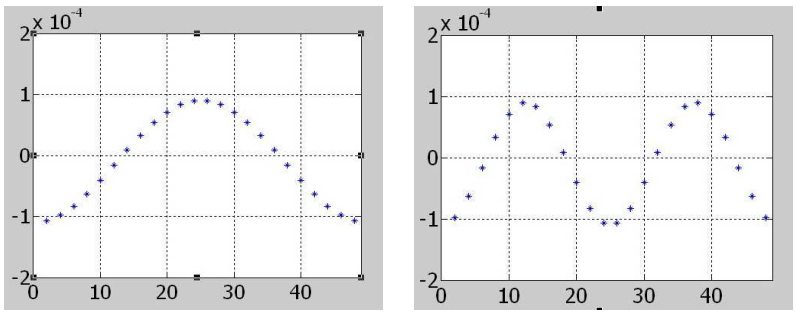

a) b)

Fig. 2. $K_A(m)$ for a high pass (a) and a bandpass (b) spatial filter.

In Fig. 2 the dispersion curves for a high pass and a bandpass spatial filter are presented.

3. Log-domain equations

In the following we briefly review the principle of mapping a set of linear state equations in the log-domain. Since the theory behind linear spatial filtering refers to autonomous systems, we consider the couple of state and output equations below.

$$\dot{X} = AX, \quad Y = CX, \tag{13}$$

where X is the M-dimensional column state vector, A is the M×M state transition matrix, C is the M dimensional row vector relating the (scalar) output Y to the state.

In a standard implementation, the natural physical significance of the state variables is usually that of voltage. However, in order to convert the system of differential equations (13) into the log-domain using CMOS transistors in week inversion, we will further assume that the physical significance of the state variables x_i is that of current.

With the following change of variable:

$$x(i) = I_S e^{\alpha v_x(i)} - x_0, \tag{14}$$

where x_0 is an offset introduced to obey elementary calculus constraints as well as to avoid static point convergence problems in the implementations equation "i" can be written in the form (15) and will have a bounded dc steady-state solution:

$$\begin{aligned} &CI_S\alpha\dot{v}_x(i)e^{\alpha v_x(i)} = A_2I_Se^{\alpha v_x(i-2)} + A_1I_Se^{\alpha v_x(i-1)} - A_0I_Se^{\alpha v_x(i)} + \\ &+A_1I_Se^{\alpha v_x(i+1)} + A_2I_Se^{\alpha v_x(i+2)} - x_0(2A_1 + 2A_2 - A_0). \end{aligned} \tag{15}$$

Dividing equation (15) by $e^{\alpha v_x(i)}$ and using the notations:

$$\begin{aligned} &C_x = CI_S\alpha,\ x_{offset} = x_0(2A_1 + 2A_1 - A_0) = I_{X_0} \\ &A_1I_S = I_{A_1},\ A_2I_S = I_{A_2},\ A_0I_S = I_{A_0}, \end{aligned} \tag{16}$$

the new state equation "i" can be rewritten as:

$$C_x\dot{v}_x(i) = CT - I_{X_0}e^{-\alpha v_x(i)} \tag{17}$$

where CT represent the coupling terms:

$$\begin{aligned} &CT = I_{A_2}e^{\alpha(v_x(i-2)-v_x(i))} + I_{A_1}e^{\alpha(v_x(i-1)-v_x(i))} + \\ &+I_{A_2}e^{\alpha(v_x(i+2)-v_x(i))} + I_{A_1}e^{\alpha(v_x(i+1)-v_x(i))} - I_{A_0}. \end{aligned} \tag{18}$$

The equation (17) represents the Kirchhoff current law for cell "i": the current through the capacitor C_x equals the sum of currents injected by the current sources nonlinearly controlled by the voltages of the neighboring cells while CT represents the

contribution of neighboring cells over the i-th cell. Each term within CT represents the nonlinear equivalent in the log domain of the voltage controlled current sources while $I_{X_0}e^{-\alpha v_x(i)}$ defines a nonlinear conductance.

4. Transistor level implementation

As it has been shown previously, (15) represents the state equation associated to cell "i" of a first order high-pass spatial filter translated into the log-domain. The structure of a pixel obtained by the nonlinear mapping of the state equations of a linear autonomous system is composed of a nonlinear conductance, four current sources exponentially controlled by the voltages of the neighboring cells, and a dc current source.

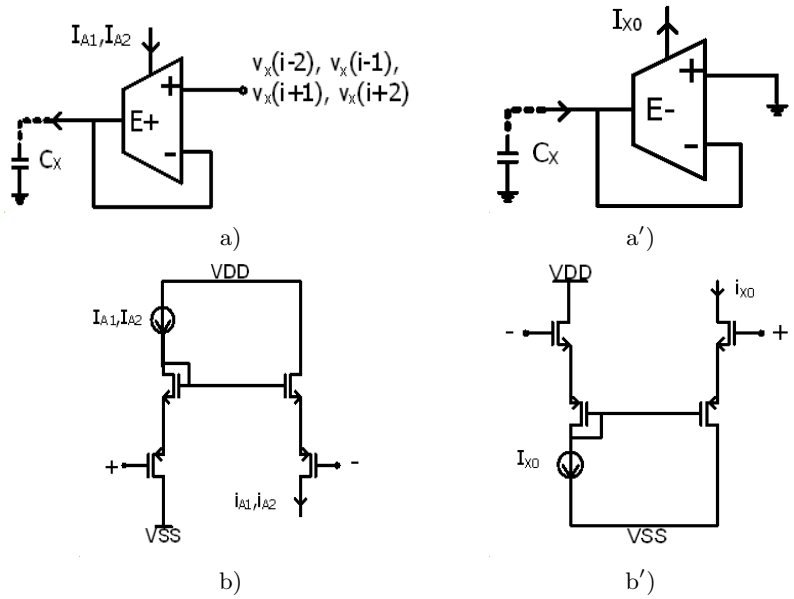

Fig. 3. a) current source exponentially controlled by the voltages of neighboring cells (injects current in cell capacitor); a′) current source exponentially controlled by the voltage of the current cell (sinks current from cell capacitor); b) transistor implementation of a); b′) transistor implementation of b).

The basic building blocks used for the implementation of the log-domain equations are shown in Fig. 3. The nonlinear controlled sources in Fig. 3 a, b, respectively 3 a′, b′ have three inputs: a current input (I_{A_1}, I_{A_2}, I_{X_0}), and two voltage inputs (v_+, v_-). The scaling factor of the sources can be controlled by an external biasing current. In this way the template coefficients and thus the spatial filtering characteristics can be modified.

Following to the above considerations, the schematic of a logarithmic cell is presented in Fig. 4 and corresponds to equation (17).

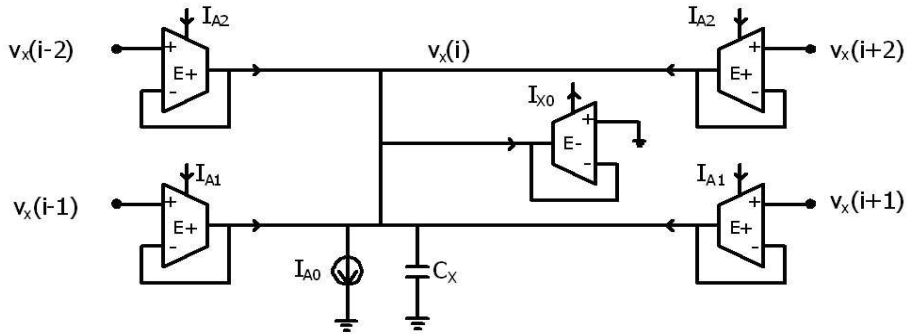

Fig. 4. Cell schematic for a low-pass/stop-band filter structure.

The above structure has been used to implement a low-pass filter for $v_x(i-2) = v_x(i+2) = 0$ and $v_x(i-1) = v_x(i+1) \neq 0$ and a stop-band filter for $v_x(i-2) = v_x(i+2) \neq 0$ and $v_x(i-1) = v_x(i+1) = 0$.

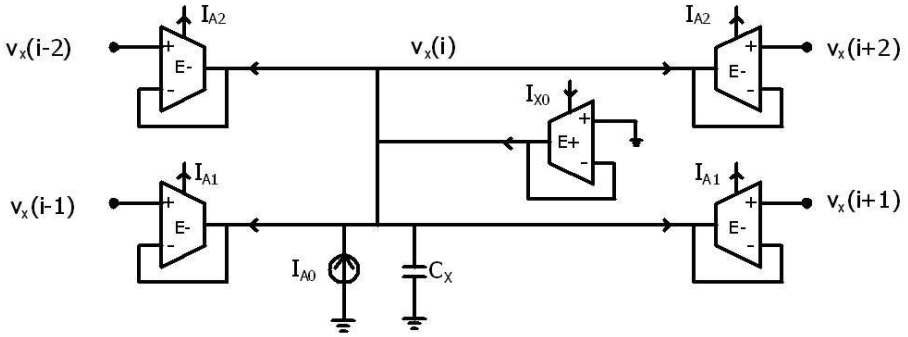

Fig. 5. Cell schematic for a high-pass/band-pass filter structure.

Multiplying equation (15) by minus one, the cell structure for a high-pass/band-pass spatial filter shown in Fig. 5 can be easily obtained.

5. Simulation results

In what follows we present the spatial frequency characteristics of a 50 cell 1D architecture configured for high-pass, low-pass, band-pass and stop-band at system level and at log-domain transistor level. For simplicity, the term A_0 has been considered zero.

In order to obtain the characteristics in Fig. 6, both the linear and the log-domain CNN have been "loaded" with a state consisting of a spatial impulse of 10 mV on one cell, all the other cells having zero state. In this way the initial condition contained all spatial frequencies with equal weights.

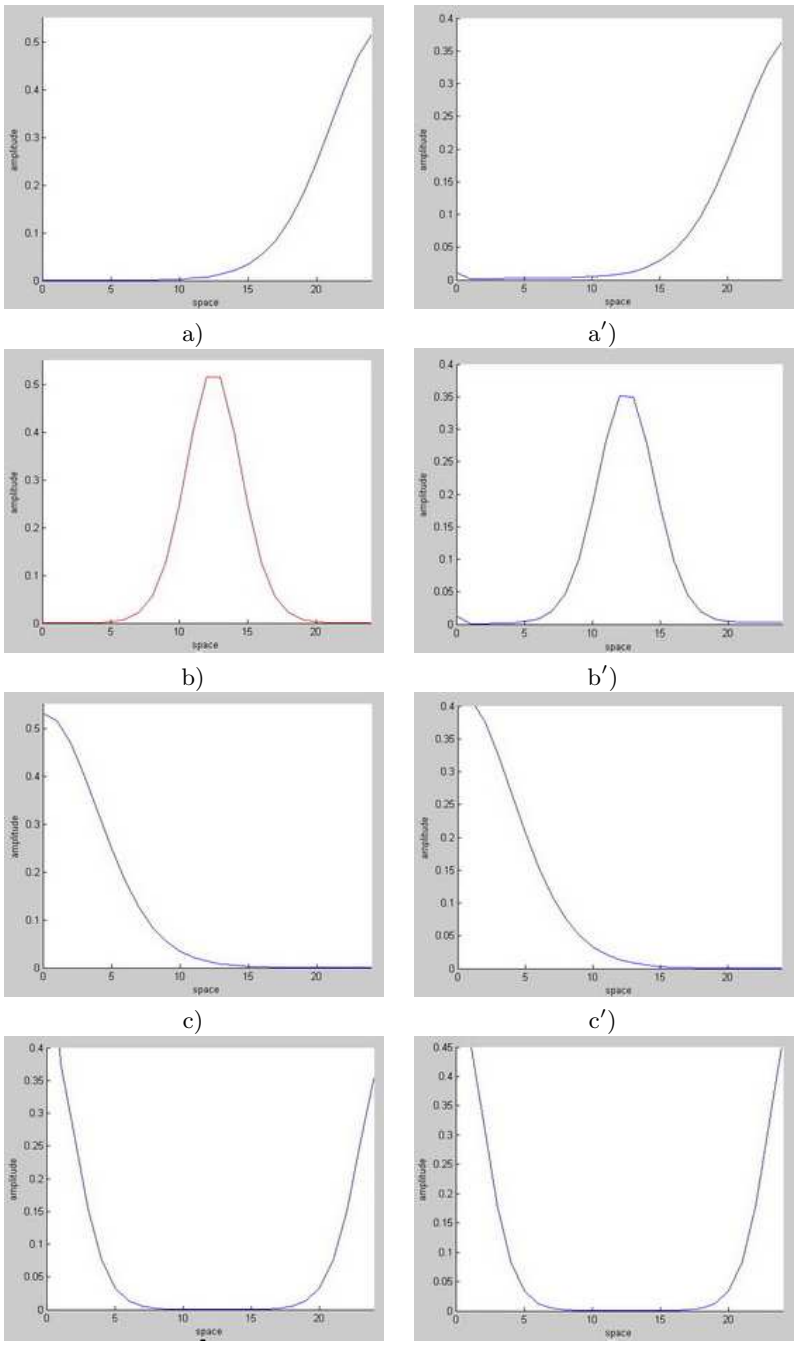

Fig. 6. High pass, band-pass, low pass respectively stop-band spatial frequency characteristics for linear OTA (a, b, c, d) and log-domain transistor level implementation (a′, b′, c′, d′).

The system level and log-domain filter parameters are presented in the table below:

Cell implementation	Filter type	Freq. characteristic	Implementation type					
			Log-domain transistor level filter				System level filter	
			Filter coefficients					
			I_{X0}	I_{A0}	I_{A1}	I_{A2}	A_1	A_2
Fig. 5	FTS	Fig. 6a/a′	2 nA	0	1 nA	0	1 ns	0
	FTB	Fig. 6b/b′	2 nA	0	0	1 nA	0	1 ns
Fig. 4	FTJ	Fig. 6c/c′	2 nA	0	1 nA	0	–1 ns	0
	FOB	Fig. 6d/d′	2 nA	0	0	1 nA	0	–1 ns

In Fig. 7 the dynamics of the time evolution of the spatial frequency characteristic for high-pass and band-pass architectures for the system level and log-domain transistor level are presented.

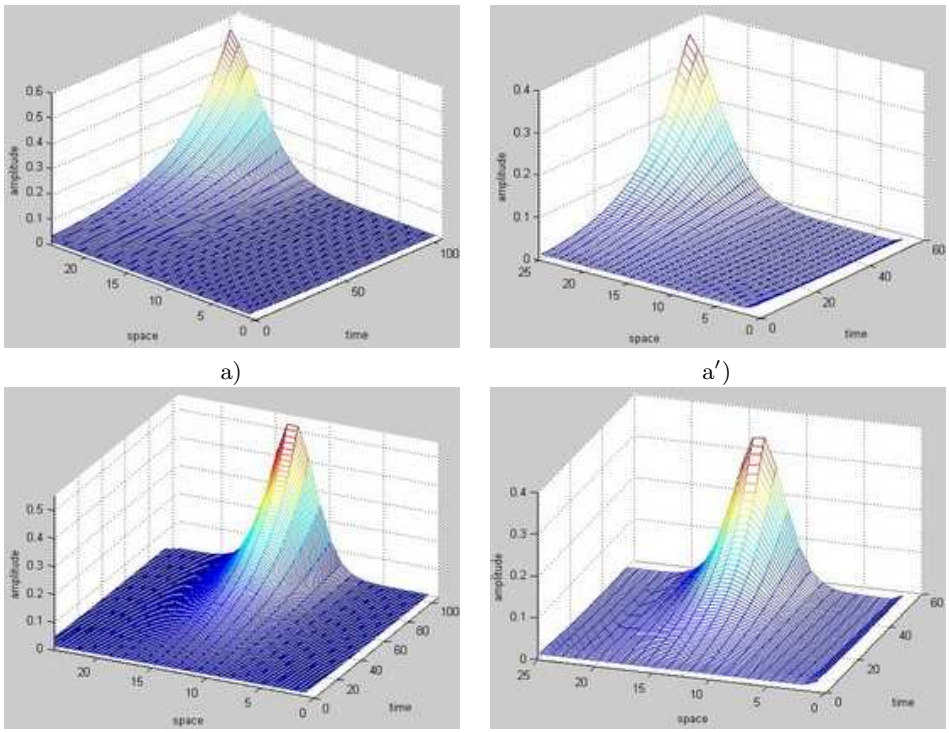

a) a′)

b) b′)

Fig. 7. Time evolution of the spatial frequency characteristics for a high-pass (a, a′) and band-pass (b, b′) CNN filter at system and log-domain transistor level respectively.

An example of edge detection using a high-pass filter realized with an ideal and log-domain architecture is shown in Fig. 8, the input state being a 10 mV amplitude square spatial signal; the transient has been stopped in both cases after 53 us. It is apparent that the responses of the two implementations are almost identical.

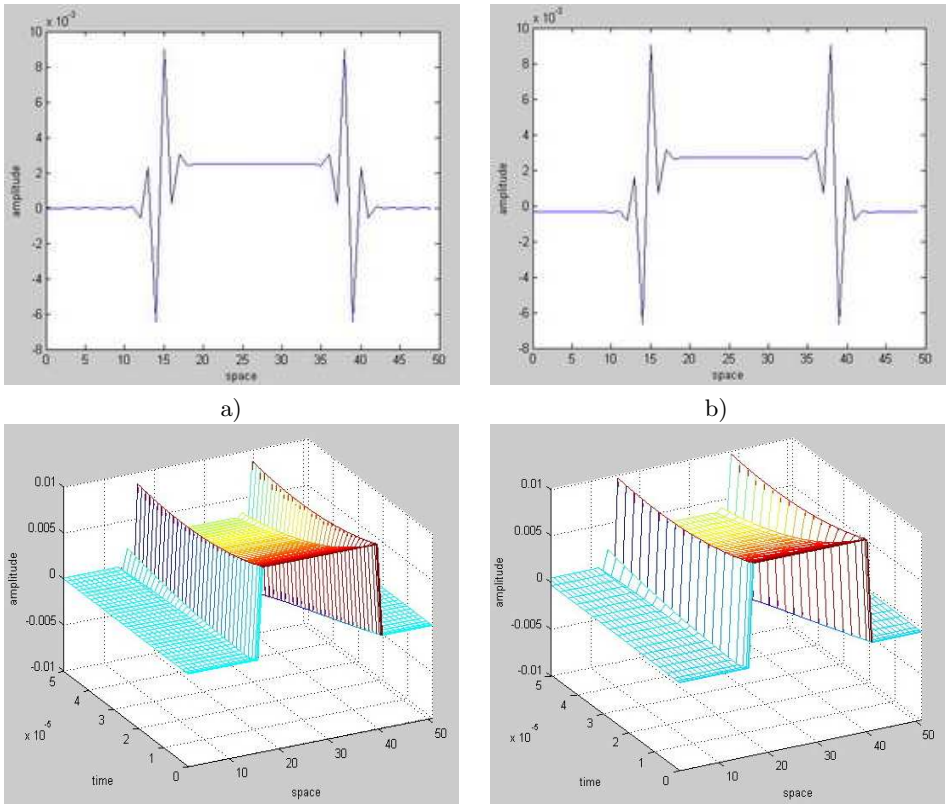

Fig. 8. Edge detection using ideal (a) and log-domain (b) implementations. Time evolution (c, d) for a square spatial input signal in both case.

6. Concluding remarks

The spatio-temporal behavior and log-domain implementation of a class of parallel analog architectures has been investigated. Among the advantages of the log-domain realization are the decrease of power consumption and silicon area aria and increase of the dynamic range while the main disadvantage is the high technological dispersion of the implementation. However, some recent results show a certain robustness of the spatio-temporal dynamics even for rather high deviations of the parameters from their nominal values. Last but not least, a significant aspect related to the design of parallel architectures using exponentially voltage controlled current sources is the need of keeping the transistors width as low as possible in order to minimize parasitic capacitance since the cell capacitance should be much higher than the parasitic capacitance of each source.

Acknowledgments. This paper has been financially supported by the Higher Education Scientific Research National Council under Grant PN2 – ID_310.

References

[1] CHUA L. O., YANG L., *Cellular Neural Networks: Theory*, IEEE Trans. Circuits Syst., vol. **35**, no. 10, pp. 1257–1272, October 1988.

[2] CHUA L. O., YANG L., *Cellular Neural Networks: Applications*, IEEE Trans. Circuits Syst., vol. **35**, no. 10, pp 1273–1290, October 1988.

[3] ROSKA T., VANDERWALLE J., *Cellular Neural Networks*, John Wiley & Sons, 1993.

[4] CHUA L. O., HASLER M., MOSCHYTZ G. S., NEIRYNCK J., *Autonomous Cellular Neural Networks: A Unified Paradigm for Pattern Formation and Active Wave Propagation*, IEEE Trans. Circuits Syst., vol. **42**, pp. 559–577, October 1995.

[5] SHI B. E., *Gabor-type filtering in space and time with cellular neural networks*, IEEE Trans.on Circuits and Syst., vol. **45**, no. 2, February 1998.

[6] ARENA P., FORTUNA L., FRASCA M., SICURELLA G., *An Adaptive, Self-Organizing Dynamical System for Hierarchical Control of Bio-Inspired Locomotion*, IEEE Transactions On Systems, Man, And Cybernetics Part B: Cybernetics, **34**, no. 4, pp. 1823–1837, 2004.

[7] GORAŞ L., CHUA L. O., *Turing Patterns in CNN's - Part II: Equations and Behaviors*, IEEE Trans. Circuits Syst, vol. **42**, pp. 612–626, October 1995.

[8] GORAŞ L., *On Pattern Formation in Cellular Neural Networks*, NATO Advanced Research Workshop, Siena, Italy, 22–24 October, 2002; published in V. Piuri , M. Gori , S. Ablameyko and L. Goraş, (editors) *Limitations and Future Trends in Neural Computation*, Volume **186**, NATO Science Series: Computer & Systems Sciences.

[9] TEODORESCU T., GORAŞ L., *On the Dynamics of Turing Pattern Formation in 1D CNN's*, Proc. SCS'97, Iaşi, pp. 109–112, October 1997.

[10] GORAŞ L., CHUA L. O., *On the Role of CNN Initial Conditions in Turing Pattern Formation*, Proc. SCS'97, pp. 105–108.

[11] GORAŞ L., CHUA L. O., *On the Influence of CNN Boundary Conditions in Turing Pattern Formation*, Proc. ECCTD'97, Budapest, pp. 383–388, 1997.

[12] GORAŞ L., ALECSANDRESCU I., VORNICU I., *Spatial filtering using linear analog parallel architectures*, International Symposiunm on Signals, Circuits and Systems ISSCS 2009, Iaşi, Romania.

[13] RODRIGUEZ-VAZQUEZ A., SERRANO-GOTARREDONA T., O*n the design of second order dynamics reaction-diffusion CNNs*, Journal of VLSI Signal Processing, **23**, pp. 351–371, 1999.